Name: _____

5.08 Final Exam

This exam is worth **200 points**.

This final exam contains **24 pages.**
The last page is an Appendix.
Check that you have all pages before commencing the exam.
Read all questions, figure captions, and figures carefully.
Write neatly – what cannot be read or deciphered will not be graded.

Question 1: _____ / **40 pts**

Question 2: _____ / **60 pts**

Question 3: _____ / **20 pts**

Question 4: _____ / **40 pts**

Question 5: _____ / **25 pts**

Question 6: _____ / **15 pts**

TOTAL: _____ **/ 200 pts**

1. (**40 pts total**) We closed the synthase module with a discussion of the enterobactin synthetase. Recall that the non-ribosomal peptide enterobactin is an iron chelator or "siderophore" employed by bacteria for the acquisition of this essential nutrient. Several natural products with structures similar to enterobactin have been isolated from other organisms, including *Paenibacillus elgii* B69. One of these siderophores is shown below (*Environ. Microbiol.* **2011**,*13*, 2726-2737).

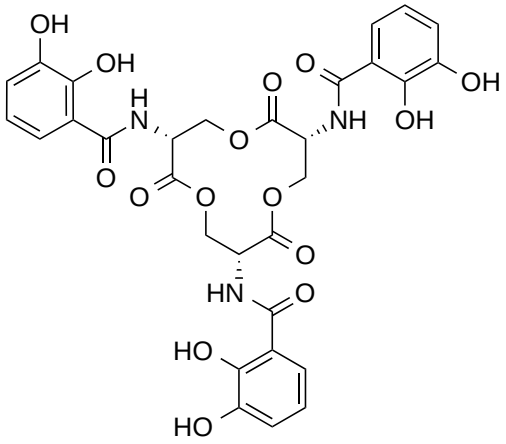

Enterobactin (Ent)

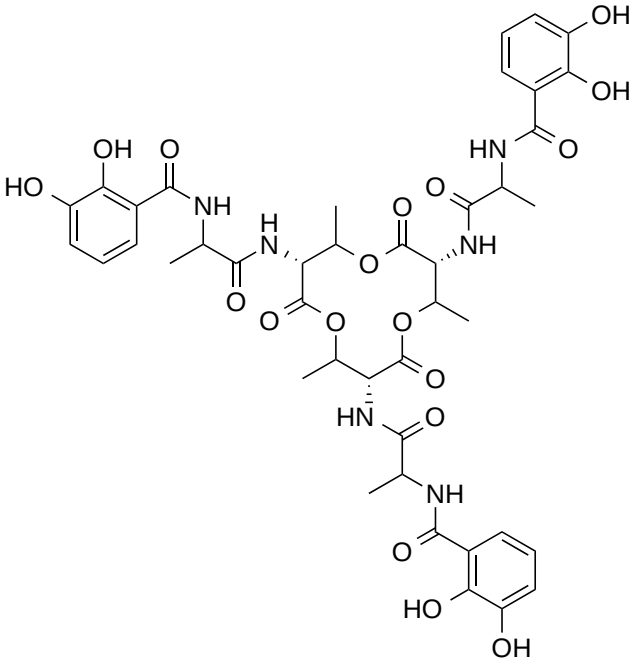

Siderophore from *P. elgii*

(a) (8 pts) Draw the monomeric building blocks used in the biosynthesis of the siderophore from *P. elgii*.

(b) (2 pts) How many C domains will the assembly line for the *P. elgii* siderophore contain?

(c) (15 pts) Using your knowledge of enterobactin biosynthesis as a guide, propose the biosynthesis of the siderophore from *P. elgii*. Include a cartoon of the assembly line with the monomers loaded onto the appropriate carrier proteins.

(d) (5 pts) Draw the species tethered to the final domain of this module right before product release and indicate the mechanism of product release.

(e) (10 pts) The genome sequence of the bacterium *P. elgii* B69 was released in 2011 and this information enabled bioinformatic analyses to identify the gene clusters responsible for the production of many natural products, including the siderophore presented above. The genus name *Paenibacillus* translates to "almost *Bacillus*" (*paene* is Latin for "almost"), and *Bacillus* is a related bacterial genus. It was noted that the gene cluster identified for the *P. elgii* siderophore has many similarities to a previously identified gene cluster from *Bacillus* spp., including *B. anthracis*, the causative agent of anthrax. These *Bacilli* produce a siderophore named bacillibactin. This siderophore is structurally related to the *P. elgii* siderophore and enterobactin as shown below.

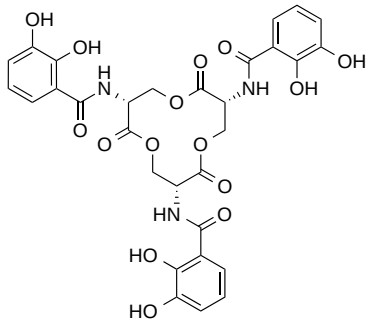

Enterobactin (Ent)

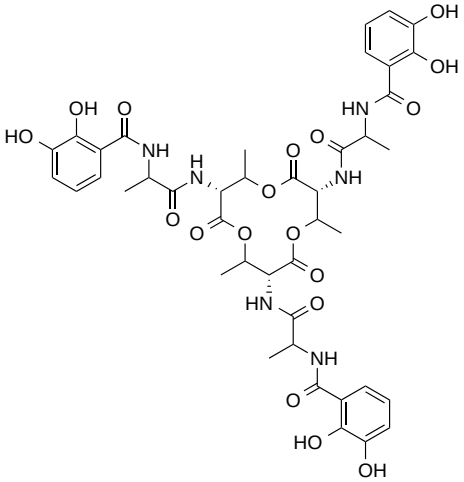

Siderophore from *P. elgii*

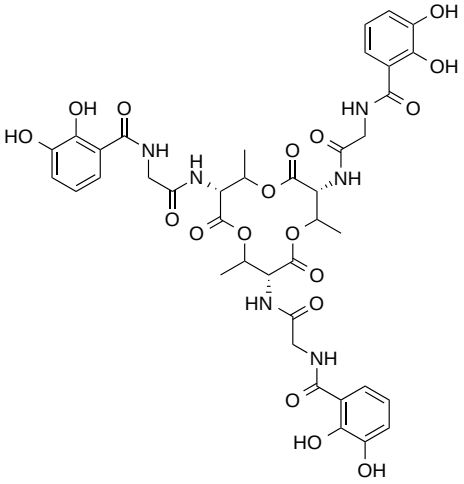

Bacillibactin from *Bacillus* spp.

(i) A phylogenic analysis indicated that the gene cluster for production of the *P. elgii* siderophore evolved from an ancestral bacillibactin biosynthetic gene cluster of *Bacillus*. Using your knowledge of NRPS biosynthesis and the siderophore structures, present a hypothesis for how the *P. elgii* cluster evolved. In other words, what change(s) was necessary to enable production of the new siderophore?

(ii) Propose an experiment to test your model. Be brief.

2. (**60 pts total**) In addition to the action that takes place in the decoding center of the ribosome, other molecular interactions between the ribosome and various translation factors and tRNAs occur and contribute to the overall translation process. A number of structural studies of the prokaryotic 70S ribosome in complex with other components of the translation machinery, such as tRNAs and release factors, indicate that helix 69 (H69) of the 23S rRNA interacts with these components. This question examines some recent **pre-steady state kinetic studies** that were performed to help address how H69 of the 23S rRNA contributes at various stages of the translation cycle (*J. Biol. Chem.* **2011**, *286*, 25604-25610).

On the basis of prior studies, the researcher studied two mutant ribosomes: a G1922A mutant and an A1913U mutant. The researchers used these ribosomes to study whether these mutations in H69 affect (i) tRNA selection and (ii) release factor selection. A schematic of H69 is shown below in **Figure 1**.

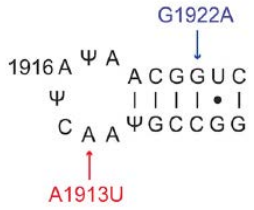

Figure 1. Schematic of helix 69 (H69) of the 23S rRNA indicating the mutation sites. The ψ symbol indicates pseudouridines. G1922 is located in the base of the H69 stem. A1913 is located in the H69 loop region.

The kinetic model for tRNA selection we studied in class and recitation is provided below for reference.

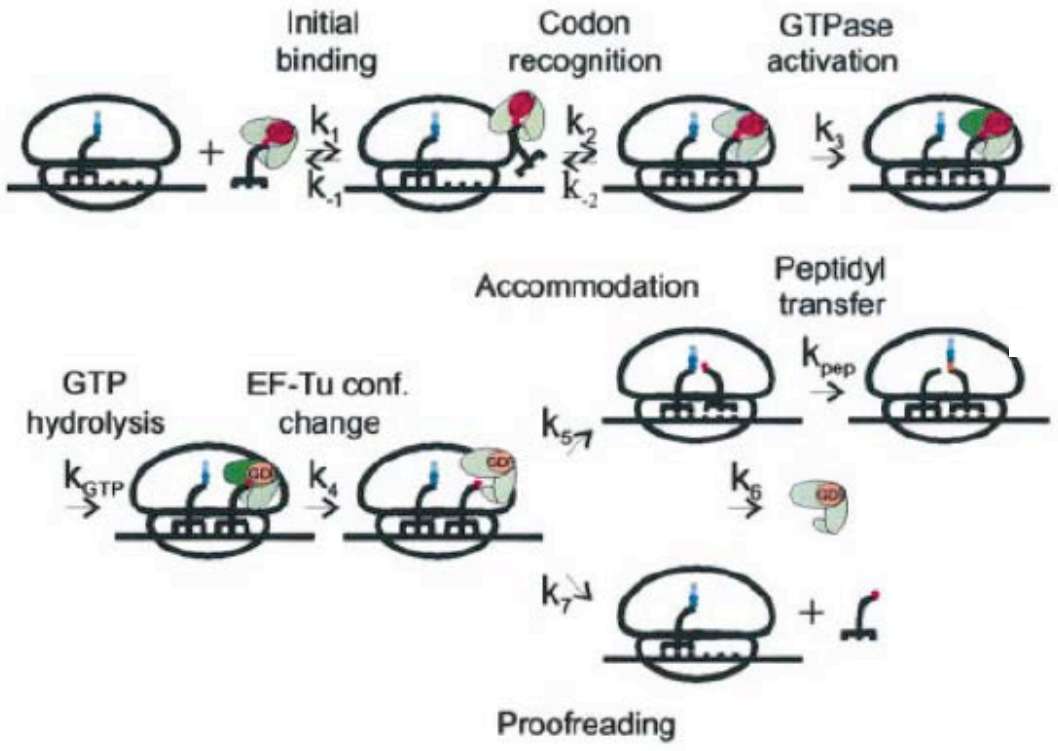

Figure 2. Kinetic model for EF-Tu delivery of aa-tRNA^{aa} to the A site of the ribosome.

In **experiment #1**, the researchers examined the effect of H69 mutations on GTP_{ase} activation. Recall from class and recitation discussions of the kinetic model presented in **Figure 2** that conformational changes are rate-limiting; the rate of GTP hydrolysis (K_{GTP}) is limited by GTP_{ase} activation (k_3). Thus, the researchers determined the rate of GTP hydrolysis by EF-Tu ternary complexes as a proxy for GTP_{ase} activate in the presence of wild-type, G1922A, and A1913U ribosomes. The researchers observed no substantial differences in the rates of GTP hydrolysis for these three ribosome species and the EF-Tu•GTP•aatRNA^{aa} complexes studied. (**Data not shown**)

In **experiment #2**, the researchers focused on the accommodation step. Because the conformational change associated with accommodation (k_5) is rate limiting for peptide bond formation (k_{pep}), the researchers monitored peptide bond formation as a proxy for accommodation. In this experiment, initiation complexes of wild-type and mutant ribosomes were prepared with fMet-tRNA^{fMet} in the P-site and an empty A site. A synthetic mRNA with the coding region AUG-XXX-UUU was employed where XXX corresponds to the triplet codon in the A site. Several different XXX codons and tRNAs were examined. The rate of dipeptide formation was monitored following rapid mixing of the ribosomes with EF-Tu ternary complexes. The resulting data are presented in **Figure 3.**

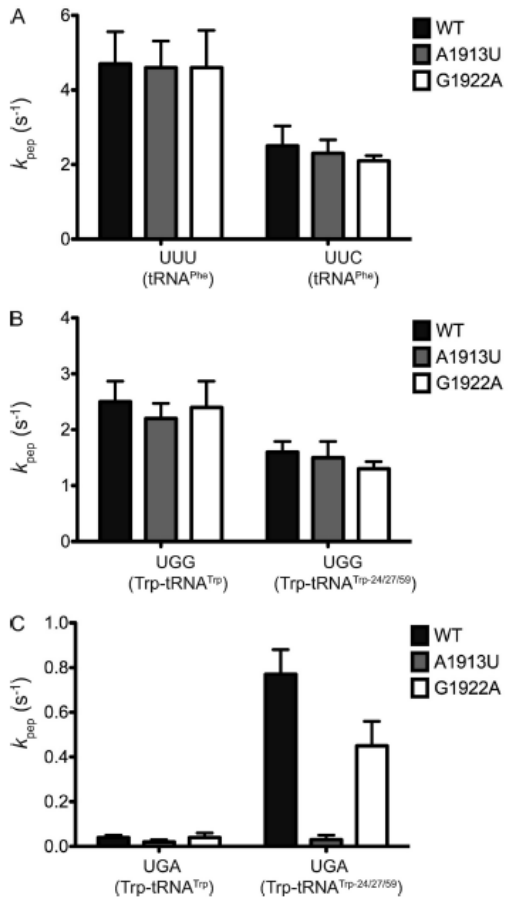

Panel A:

UUU and UUC are codons for Phe.

tRNA^{Phe} indicates that Phe-tRNA^{Phe} was employed.

Panels B and C:

UGG is a codon for Trp.

UGA is a near-cognate codon for Trp. It is also a stop codon.

Trp-tRNA$^{Trp-24/27/59}$ is a miscoding tRNA that can accommodate certain near-cognate triplet codons.

Figure 3. Effect of H69 mutations on tRNA accommodation. Observed rate of peptide bond formation (k_{pep}) for formation of dipeptides. The labels under the bar plots indicate (i) the codon in the A site and (ii) the aa-tRNA^{ss} evaluated. Further details are given to the right of the data panels.

In **experiment #3**, the researchers examined the rate of peptide bond formation (i.e., accommodation) for several codons that we can consider to be special because the decoding of these codons depends on non-canonical wobble position. These experiments were performed like those in **experiment #2** except that a different set of synthetic mRNAs and aatRNA^{aa} were employed. The data are presented in **Figure 4.**

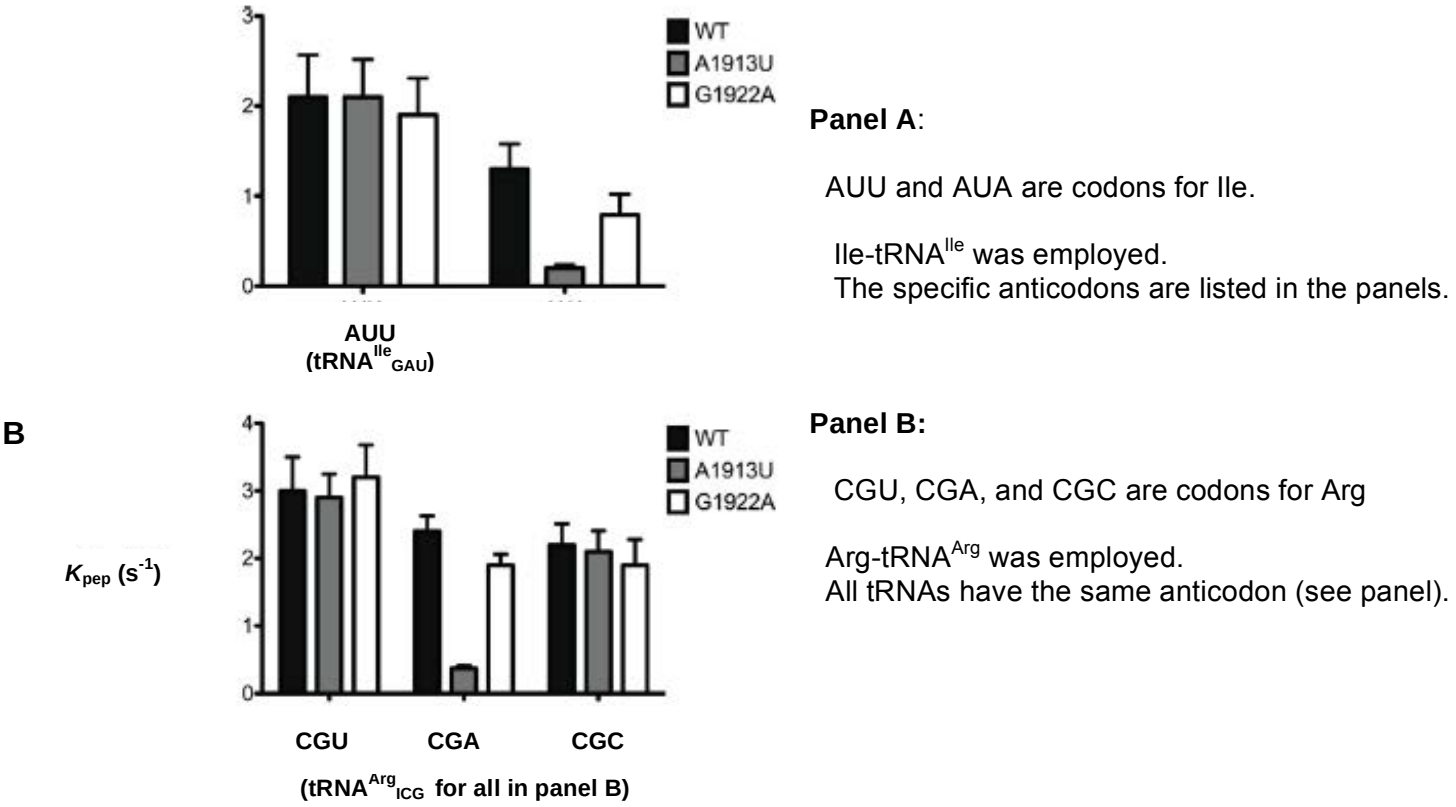

Panel A:

AUU and AUA are codons for Ile.

Ile-tRNA^{Ile} was employed.
The specific anticodons are listed in the panels.

Panel B:

CGU, CGA, and CGC are codons for Arg

Arg-tRNA^{Arg} was employed.
All tRNAs have the same anticodon (see panel).

Figure 4. Further studies of the effect of H69 mutations on tRNA accommodation. The labels under the bar plots indicate (i) the codon in the A site and (ii) the aa-tRNA^{ss} evaluated. Further details are given to the right of the data panels. Note that some of the tRNAs contain modified bases in the anticodon region.

In **experiment #4**, the researchers examined the effect of H69 mutations on stop codon recognition. Recall that RF1 and RF2 are release factors that recognize various stop codons in the A site and catalyze peptide release. In this experiment, the researchers prepared ribosome complexes where [^{35}S]-fMet-tRNA^{fMet} was in the P-site. The synthetic mRNA contained AUG-XXX-UUU where XXX is a stop codon (UAA, UAG, UGA). The ribosomes were rapidly mixed with saturating amounts of RF1 or RF2 and the rate of peptide release (k_{rel}) was monitored using the ^{35}S radiolabel. The resulting data are presented in **Figure 5.**

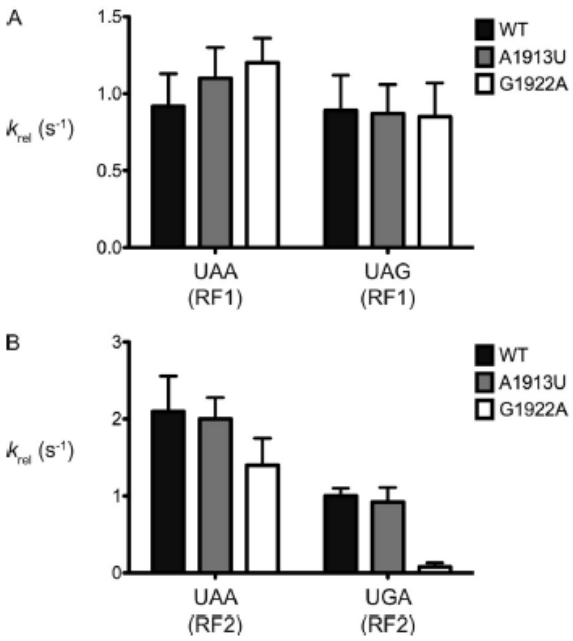

Figure 5. Effect of H69 mutation on stop codon recognition. Rate of peptide release for RF1 (panel A) and RF2 (panel B) for wild-type and mutant ribosomes.

(a) (5 pts) This study required mutant ribosomes. Briefly explain how you would obtain and purity the mutant ribosomes required for this study.

(b) (5 pts) Draw and label the initiation complex used in these studies.

(c) (5 pts) These pre-steady state kinetics experiments used rapid mixing. Draw a schematic for the apparatus required for experiments investigating tRNA delivery by EF-Tu and indicate the components of each syringe required to initiate the reaction. You can assume that the ribosome initiation complexes are pre-assembled and that the aa-tRNA^{ss} are charged with the appropriate amino acid. You need not include how the reaction is stopped or quenched.

(d) (10 pts) What do the data from **experiment #1** tell you?

(e) (20 pts) What do the data from **experiments #2 and #3** (**Figure 3 and 4**) tell you? Be sure to address the data provided in all panels in your answer.

(f) (10 pts) What do the data from **experiment #4** (**Figure 5**) tell you?

(g) (5 pts) Taking the observations from **experiments 1-4** together, briefly describe how H69 contributes to the translation cycle.

Problem 3 (20 points): In eucaryotes, deubiquitinases (DUBs) remove ubiquitin conjugates from a diverse range of protein substrates altering their stability, localization and activity. One of the deubiquitinases named USP19 is involved in deubiquitinating PCNA, the sliding clamp and processivity factor that plays a crucial role in DNA replication and repair. USP19 is a protease that hydrolyzes amide linkages and has an essential cysteine in its active site. Two assays have been developed to monitor the activity of USP19 using two artificial substrates Ub-CONH-Ub (diUb) and UbCONH-AFC **(Figure 1A).** In the first assay the reaction can be monitored by SDS-PAGE and Commassie blue staining (**B**) and in the second assay the AFC released is fluorescent(**C**).

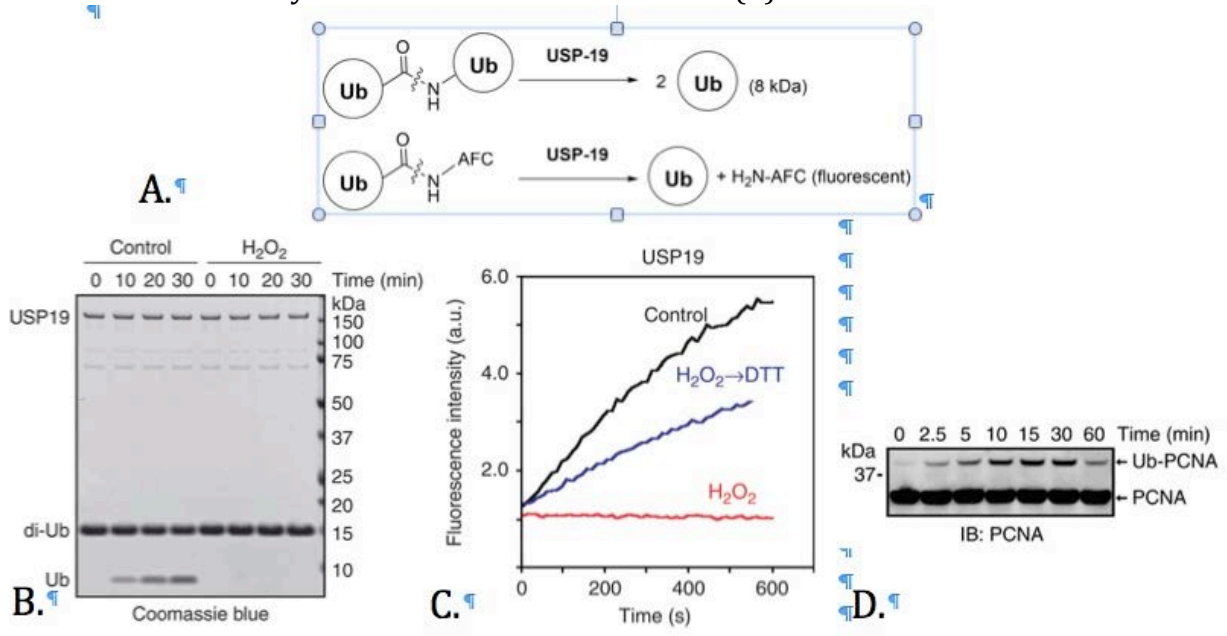

Figure 1. **A**. Two artificial substrates have been developed to assay for the deubiquitination by USP19. **B**. In the top assay in A, the reaction is monitored by SDS PAGE. **C**. In the bottom assay in A, the reaction is monitored by fluorescence changes. **D**. The protein PCNA is monitored by SDS PAGE and western blotting using an antibody to PCNA.

An hypothesis has recently been put forth that an essential response to oxidative stress which results in DNA damage is the control of the ubiquitination state of PCNA. Several experiments have recently been reported in an effort to understand how this regulation occurs. First the assays in **Figure 1A** were used to monitor the activity of DUB (USP19) thought to be important in the deubiquitination of PCNA. The results are shown in **Figure 1 B and C** as are the effects of H_2O_2 and DTT (dithiothreitol, structure in the Appendix I) on the activity of USP19.

1. (**2 points**) State two essential features of ANY system that is regulated by post-translational modification (PTM).

2. (**6 points**) What do the data in Figure 6 B and C tell you?

3. **(2 points)** What is a PTM that might explain these results? Show the structure and chemistry of its formation.

4. (**6 points**) i. What reagent(s) might you use to determine if this signaling is important inside the cell? State in one sentence why you chose this reagent and one issue that might be encountered by its use .

ii. Show the chemical mechanism by which the reagent modifies the PTM-protein.

5. (**4 points**) There are many ways to generate the small molecule that is ultimately responsible for the PTM identified in part 3. One of these is the NADPH oxidases (NOX proteins).
i. What is the reaction catalyzed by these proteins?

ii. What are the cofactors of the protein required and what is unusual about their role compared to the role of these same cofactors in other proteins?

Problem 4 (40 points) The purine pathway in mammals requires 10 steps and six enzymes to produce IMP from PRPP (**see Appendix**). The pathway branches from IMP to produce GMP and AMP, each pathway involving two steps (Eq 1 for IMP to GMP). The second step of this pathway that involves conversion of XMP to GMP, requires both ATP and glutamine and generates AMP and PPi. (Eq 1).

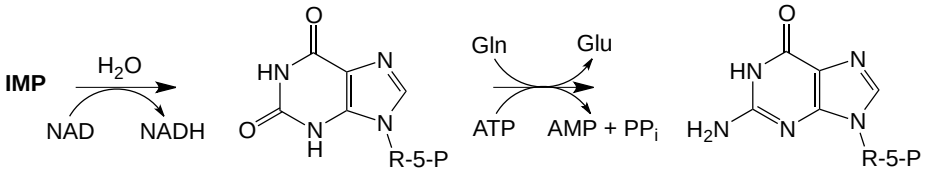

Eq 1

The Benkovic lab proposed that the purine biosynthetic pathway is organized into "purinosomes". This proposal was based in part on the use of fluorescently tagged enzymes in the pathway that were transiently transfected into different cell types and monitored using fluorescence microscopy under purine depleted (P-) and purine-replete (P+) growth conditions. Recently, several additional experiments have been carried out in an effort to provide further support for this clustering model.

In one set of experiments a new method called ^{1}H NMR metabolite scanning that allowed monitoring of 48 metabolites was used. The differences in some of the intracellular purine levels in the two growth conditions is shown in **Figure 1**.

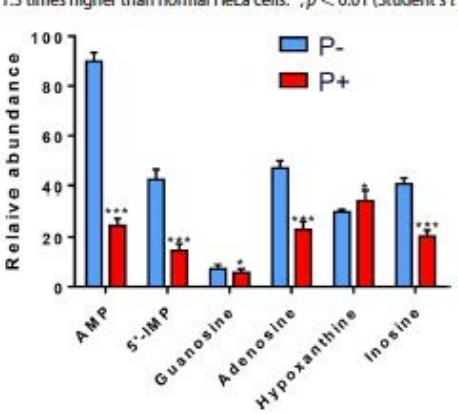

Figure 1 Relative abundance of intracellular purines in ^{1}H NMR metabolite scanning in HeLa cells cultured in purine-depleted and purine-replete medium. Data are the average of 10 experiments.

In a second set of experiments, Hela cells were grown in purine depleted and purine-replete media, pulsed with [^{15}N]-glycine, and the incorporation of a ^{15}N into IMP, AMP and GMP was measured over time and calculated by dividing the amount of [^{15}]N-IMP (or AMP

or GMP) by the amount of monoiostopic [^{15}N,^{12}C]- and [^{14}N,^{12}C]-nucleotide. The flux was estimated by calculating the initial incorporation rate of ^{15}N into the NMPs. The results are shown for IMP in **Figure 2A** and AMP in **Figure 2B**. The results for GMP are not shown, but are similar to those shown for AMP **(Figure 2B)**.

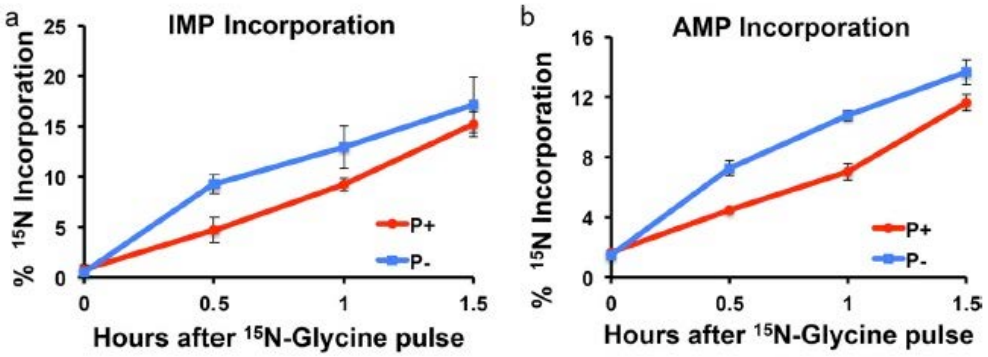

Figure 2. Incorporation of [^{15}N]-glycine into IMP and AMP. **A**. The incorporation of [^{15}N]-glycine into IMP. The incorporation was plotted using percentage of ^{15}N incorporated purines as a function of time of incubation. HeLa cells cultured in depleted media (in blue) and in P-replete media (in red) over 1.5 h. The initial incorporation rate for IMP, AMP, and GMP was calculated according to the slope of the linear relationship of the incorporation plot within 1 h. **B.** The incorporation of [^{15}N]-glycine into AMP. The incorporation of [^{15}N]-glycine into GMP is similar to AMP and the data is not shown.

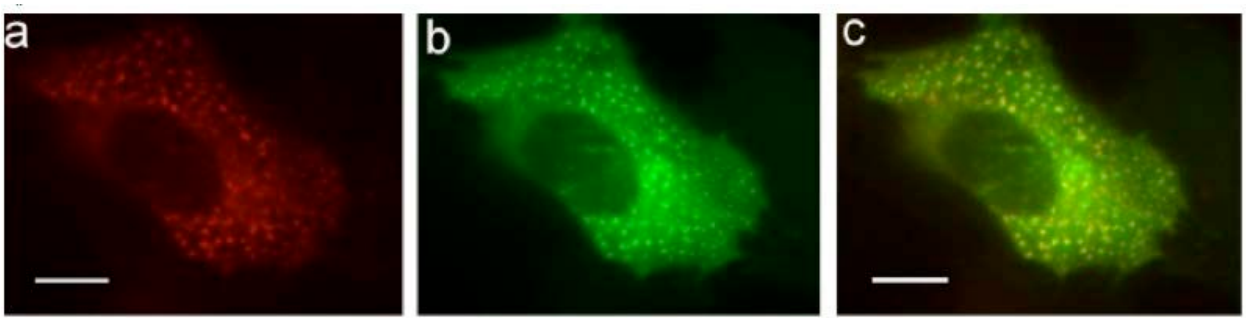

Figure 3. HeLa cells were co-transfected with GMP synthetase fused to green fluorescent protein (GMP-GFP) and with FGAMS-OFP (FGAM synthetase the fourth enzyme in the pathway) and grown in purine-depleted media. In panel **a**, FGAMS-OFP was transfected and in panel **b,** GMP-GFP was co-transfected with FGAMS-OFP. Panel **c** is the merged image. The scale bar is 10 micrometers.

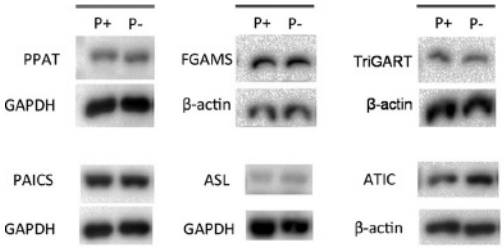

Figure 4. Western blot analysis of enzymes in the purine biosynthetic pathway in HeLa cells grown under P, replete (P+) and purine, depleted (P,) cells. Quantification of protein expression levels from three independent blots was determined by calculating the optical density of the target blot. GAPDH and actin were used as the loading control.

The results in **Figure 1 and 2** suggested an additional experiment might provide new insight about the enzymes found in the purinosome. GMP synthetase was fused to GFP (GMP-GFP). In **Figure 3A** HeLa cells transfected with FGAMS-OFP (see Appendix for pathway) were grown in P- media, whereas in **Figure 3B**, both GMP-GFP and FGAM-OFP were transiently transfected into the cells. **Figure 3C** is a merge of data. In a final control experiment, western blots were carried out on HeLA cells grown under replete and depleted purine growth conditions (**Figure 4**).

Questions (40 points)

GMP synthetase (Eq 1) is a two domain protein. One domain is a member of the amidotransferase superfamily of enzymes distributed widely in Nature and its second domain is a member of the PurM (AIRS in Appendix) superfamily.

i. **(5 points)** Propose a chemical mechanism for the role of glutamine in this reaction and of all amidotransferases.

ii. **(5 points)** Propose a role for the PurM domain of GMP synthetase showing the common ATP chemistry.

iii (5 points) Draw a cartoon structure of the two domains in GMP synthetase and how they are connected in "all" amidotransferases.

iv (5 points) Interactions between the enzymes in de novo biosynthesis are proposed to be important because of the number of "unstable" intermediates in this pathway. The product of the first enzyme in this pathway (Appendix) is phosphoribosylamine. Show with chemical structures the basis for its instability.

v (5 points) Fluorescence microscopy and fluorescently tagged enzymes played an important role in the proposed importance of the purinosome and its assembly and disassembly. Several new types of experiments described in the Figures above were pursued to further support the importance of enzyme clustering in cells. In the results shown in **Figures 1, 2A** and **2B**, describe in one sentence each, three observations from the data that support the Benkovic model.

vi (5 points) In one sentence describe the data in Figure 3 **a** through **c**. In a second sentence describe how these data support or refute the model.

vii (5 points) Figure 4 reports the results of the western analysis of Hela cells grown under purine replete or depleted media. In one sentence describe what you see. In a second sentence describe why the results of this experiment may be important relative to the data in **Figures 1, 2A and 2B**.

viii (5 points) Comment on the clustering proposal (purinosome formation) and its advantages in metabolic pathway control.

Problem 5 (25 points) *Staphyloccus aureus* is a pathogenic organism that has the ability to colonize in almost all tissues in humans. Resistance of these organisms to current antibiotics has engendered an outcry for new strategies and targets for antibiotic development. Iron is essential for this organism and it has evolved many ingenious ways to acquire it from all kinds of environments. Nutrient limitation has thus become of interest as a potential new way to limit the organism's viability.

1 **(5 points)** Draw a clearly labeled cartoon (no chemical structures required) of the peptidoglycan and plasma membrane of a gram positive organism using *S. aureus* as a model. In this cartoon, clearly show **two** major mechanisms that this organism has evolved (using circles and squares to define protein structures) to acquire iron. Show the oxidation state of the iron and the organic molecules to which it is bound (again, the detailed chemical structure is not required).

2. (2 points) Despite iron's abundance in the earth's core and crust, its acquisition has required invention of many ingenious acquisition methods by all organisms. Why is iron difficult to obtain, despite its abundance?

3. **(8 points)** There are now known to be > 500 siderophores that bacteria synthesize as one way to tackle the problem of iron acquisition. *S. aureus* makes two distinct siderophores, the structure of one, staphyloferrin A (Fe-SA), is shown in **Figure 1**.

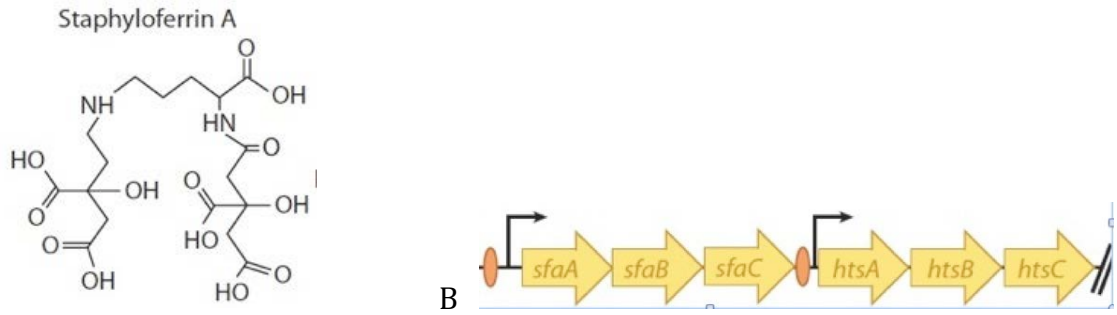

Figure 1. **A**. The structure of staphyloferrin A. **B.** Genes and their organization for the biosynthetic (*staABC*) and uptake (*htsABC*) pathway for staphyloferrin A . In addition, FhuA, an ATPase, is required for the Hts machinery to function.

Recently the structure of the HtsA in complex with iron-staphyloferrin (Fe-SA) was obtained and is shown in **Figure 2**. In the structure of HtsA, the N-terminal 35 amino acids were removed which contains Cys at residue 22 that is attached to a farnesyl group (think about terpene biosynthesis) which anchors the protein to the plasma membrane. The binding constant (K_d) of the Fe-SA to HstA was determined using a fluorescence titration method. The experiments were carried out on 15 nM HtsA in 50 mM Hepes (pH 7.4) with the excitation wavelength set at 280 nm and the emission wavelength set at 334 nm. The concentration of the Fe-SA was varied from 0.22 to 260 nM. Using this method, the K_d for Fe-SA binding to HtsA was reported to be at or below the low nM range.

i. **(4 points)** Explain the basis for the fluorescence assay and what limits its successful use.

ii. **(4 points)** Given the available information, can a K_d be measured? Why or why not?

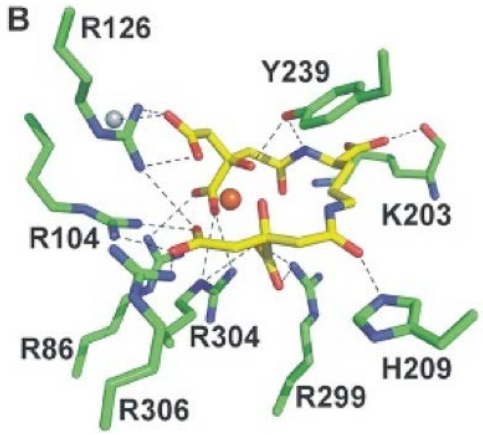

Figure 2. The first structure of a gram positive siderophore binding protein, lipoprotein, HtsA.

To further understand the interaction of Fe-SA with HtsA, mutants of HtsA were generated and an exact gene replacement was carried out to make new *S. aureus* strains. Each strain was studied for ^{55}Fe uptake and cell growth. In cells treated with 100 nM ^{55}Fe-SA and in the case of growth assays, Fe-SA is the sole source of iron. Finally, in one strain glutamates at 110 and 250 were replaced with Ala. Studies in other organisms suggested that these residues are important for interaction with HtsBC equivalents.

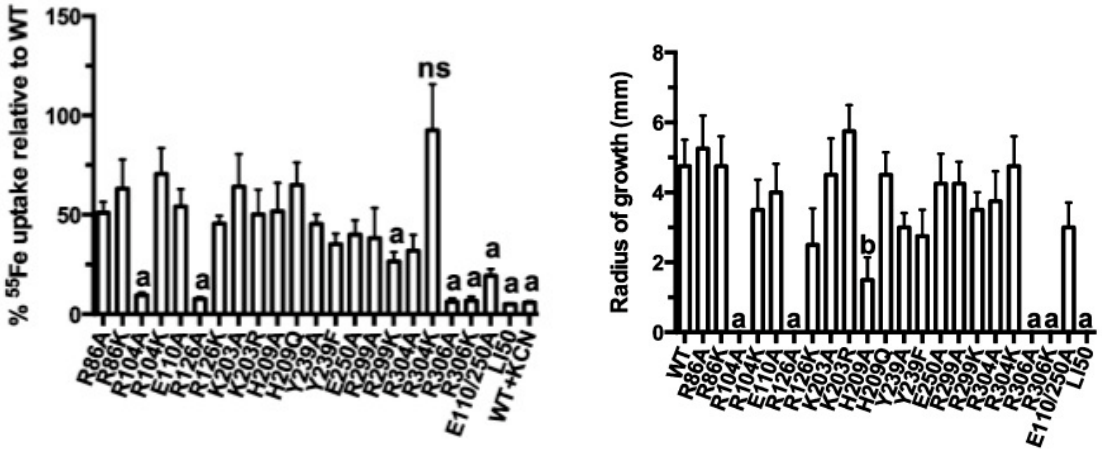

Figure 3. *S. aureus* strains containing mutations in HtsA were studied for ^{55}Fe uptake and cell growth. The symbols "a" and "b" refer to P values where P < 0.001 and < 0.05, respectively and can be ignored. "ns" is not significant.

4. (**5 points**) i. What does the data in **Figure 3A** and **3B** tell you?

ii. What is the oxidation state of the iron bound to SA? What oxidation state of iron would facilitate release from SA in the cytosol? Why?

5. (**5 points**) i. What are three reductive metabolites of O_2 that are designated as reactive oxygen species (ROS)?

ii. Which of the three is most reactive and how is "reactivity" judged?

Problem 6 (15 points). Enterocytes are the only cell type that must balance the de novo synthesis and absorption of cholesterol and the coordination of these processes in these cells has only recently (2014) been investigated. Studies on the two isoforms of Insig (Insig1 and Insig2) have been limited because of functional redundancy and neonatal lethality. Enterocytes have three sources of cholesterol: two that are shared by other cell types including the liver. To study cholesterol homeostasis in enterocytes, investigators generated mice with the intestine-specific deletion of Insig1 using Villin-Cre method in combination with germ line deletion method of Insig2 (details not important). The mice with the double deletion are designated Vil-Insig- mice and are used in the studies described below. Recall that hepcidin (the master regulator of cholesterol homoesostasis) is made in the liver which functions as a major organ for cholesterol homeostasis.

In **Figure 1** the investigators measured the protein levels of SREBP1, SREBP2 and HMGR (HMGCoA reductase) and the mRNA levels of a variety of proteins involved in lipogenic pathways.

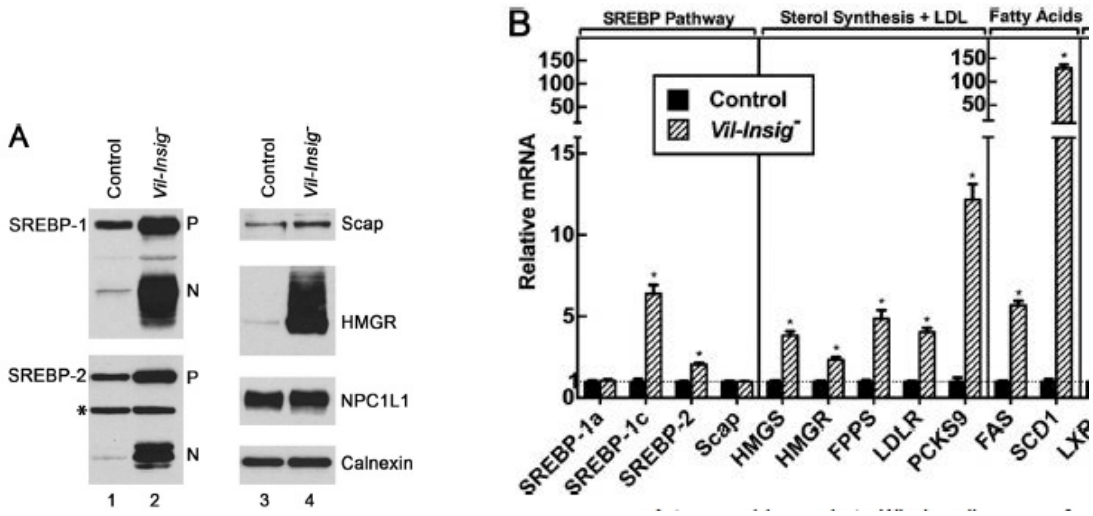

Figure 1. Protein and mRNA levels of control and Vil-Insig- mice. **A**. Lanes 1-4 measure protein levels via an immunoblot of homogeneates of control and Vil-Insig- mice. NPC1L1 and Calnexin are protein loading controls. * designates a loading control. **B**. The levels of mRNA compared with the control mice for a number of proteins involved in fat/sterol metabolism. FPPS is farnesyl pyrophosphate synthase, FAS is fatty acid synthase, SCD1 is sterol desaturase, ignore PCKS9 and LXF.

To examine the effect of intestinal lipid deficiency on in vivo lipid biosynthesis, the incorporation of intraperitonieally injected ^3H_2O into digitonin-precipitable sterols and fatty acids in control and Vil-Insig- mice were measured. The results are shown in **Figure 2.**

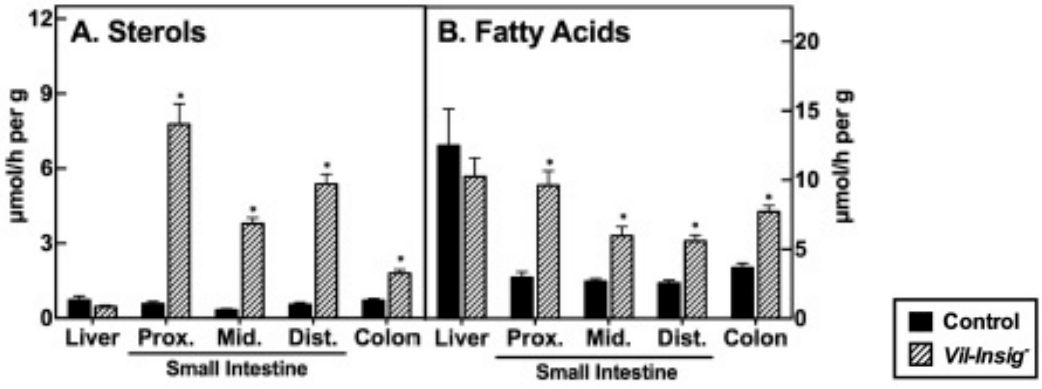

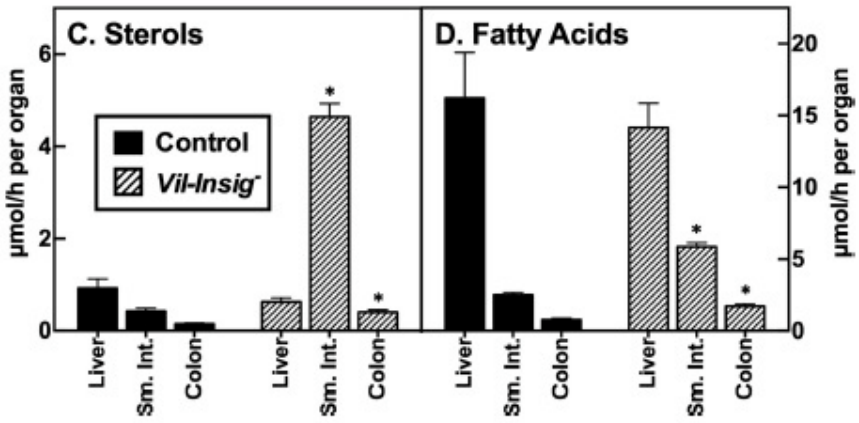

Figure 2. Control and Vil-Insig- mice (17 to 19 weeks of age, 7 mice) were injected intraperitoneally with 50 millicuries of ^3H_2O. One hour later tissues were removed and processed for isolation of digitonin-precipitable sterols (A, C) and fatty acids (B, D). The small intestine was divided into three equal length segments termed promimal (prox), middle (mid), and distal (dist). The sterol and fatty acid synthetic rates were calculated as micromoles of ^3H incorporated/h per g (A and B) or per organ (C and D) between the control and the Vil-Insig- mice.

Questions (**15 points**)

i. (**3 points**) Enterocytes are unusual in the regulation of whole-body sterol flux in that they have three sources of cholesterol. What are they?

ii. (**4 points)** Succinctly describe the results in Figure 1 and what they tell you.

3. (**4 points)** Succinctly describe the results in Figure 2 and what they tell you.

4. **(4 points)** From the data in Figures 1 and 2, do Insigs function in the enterocyte in the same fashion as other cells? What is (are) their major function? Be succinct.

Appendix I

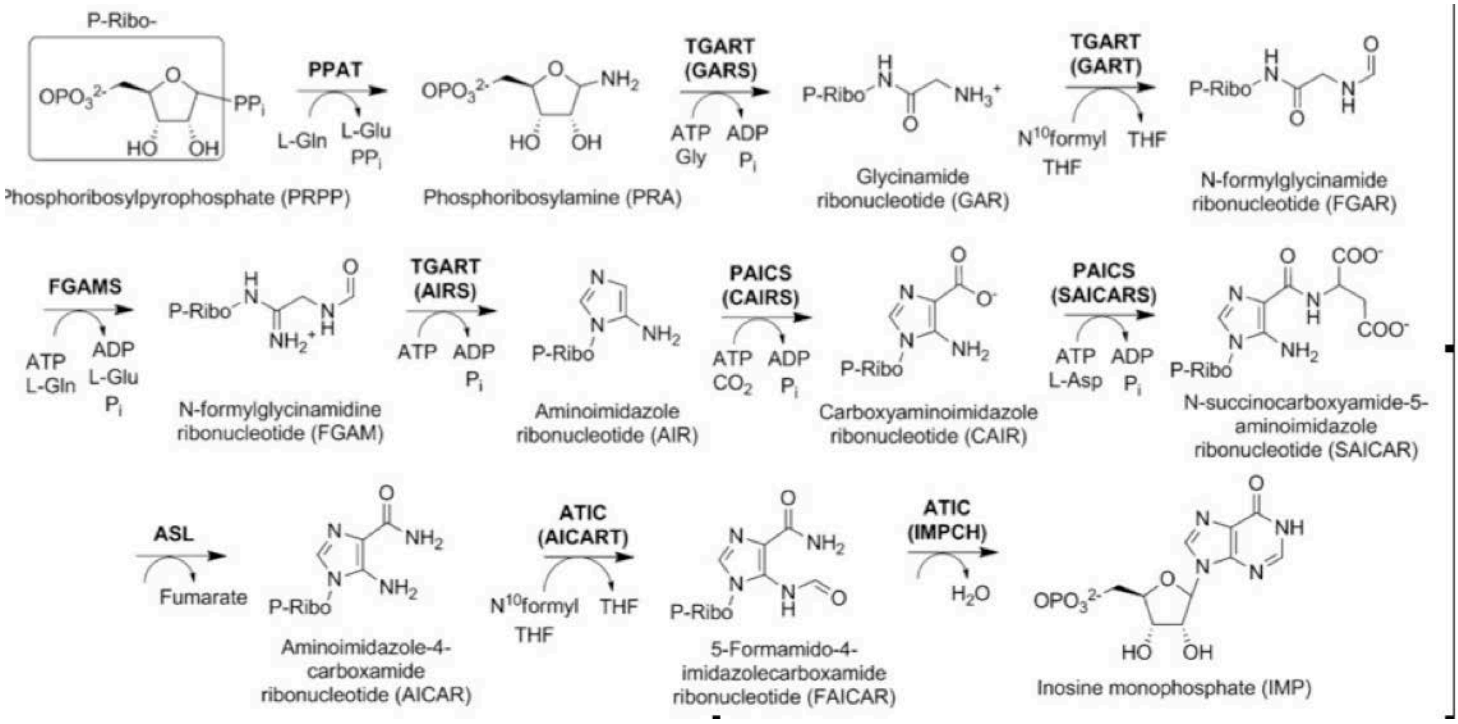

Note ADSL is another name for adenylosuccinate lyase, ASL above.

The structure of dithiothreitol 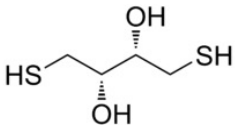

5.08J Biological Chemistry II

Spring 2016